Automatic Landmark Placement for Large 3D Facial Image Dataset

Jerry Wang
Department of Computer & Information Science
Indiana University Purdue University Indianapolis
Indianapolis, USA
jerrwang@iupui.edu

Shiaofen Fang
Department of Computer & Information Science
Indiana University Purdue University Indianapolis
Indianapolis, USA
shfang@iupui.edu

Meie Fang
School of Computer Science and Cyber Engineering
Guangzhou University
Guangzhou, China
fme@gzhu.edu.cn

Jeremy Wilson
Department of Anthropology
Indiana University Purdue University Indianapolis
Indianapolis, USA
wilsojer@iupui.edu

Noah Herrick
Department of Biology
Indiana University Purdue University Indianapolis
Indianapolis, USA
ncherric@iu.edu

Susan Walsh
Department of Biology
Indiana University Purdue University Indianapolis
Indianapolis, USA
walshsus@iupui.edu

Abstract— **Facial landmark placement is a key step in many biomedical and biometrics applications. This paper presents a computational method that efficiently performs automatic 3D facial landmark placement based on training images containing manually placed anthropological facial landmarks. After 3D face registration by an iterative closest point (ICP) technique, a visual analytics approach is taken to generate local geometric patterns for individual landmark points. These individualized local geometric patterns are derived interactively by a user's initial visual pattern detection. They are used to guide the refinement process for landmark points projected from a template face to achieve accurate landmark placement. Compared to traditional methods, this technique is simple, robust, and does not require a large number of training samples (e.g. in machine learning based methods) or complex 3D image analysis procedures. This technique and the associated software tool are being used in a 3D biometrics project that aims to identify links between human facial phenotypes and their genetic association.**

Keywords—3D facial images, landmarks, visual pattern mining

I. Introduction

Facial landmark points are critically important in many face-related applications such as facial recognition [1], craniofacial research [2], and forensic imaging. Facial landmarks can be used as reference points for face alignment or registration. They can also serve as image features or shape features in various facial analysis applications used in medical diagnoses. When these applications originate from biomedical fields, the facial landmarks often need to represent some biological or anthropological characteristics of the face, such as its morphological structure. Substantial research interest has been drawn to this challenge due to the variety and complexity of facial landmark definitions, accurate and automatic identification, and placement of facial landmarks.

Facial landmarking can be performed using either 2D images or 3D stereophotogrammetry. 2D landmarks are usually placed on 2D face images. However, this can be problematic as 2D images are sensitive to lighting and other environmental conditions; therefore, automatic placement of landmarks on 2D images is generally very unreliable [3]. In addition, 2D face images offer limited shape information, thus are often insufficient in applications that rely on capturing true 3D shape information for analysis.

Recent advances in 3D data acquisition technologies have made it possible to directly collect 3D surface images of human faces, along with their matching 2D texture images. Directly picking landmark points on a 3D surface seems the obvious course of action; however, it is very difficult, even for experienced users, as it is intrinsically unintuitive for users using a 2D screen to place the point easily and accurately. Common practice is to first define these landmarks on 2D texture images associated with the 3D face, and then inversely map these points onto the 3D surface. Although manually picking landmarks on 2D texture images can be quite accurate for experienced users, doing so for a large number of facial images is extremely time consuming and error-prone. For example, the landmarking of a single face by hand might take hours. For some machine learning applications that require hundreds and even thousands of 3D face images, manual landmark placement is impractical. In addition, maintaining the accuracy of manually picked landmarks across many faces is difficult to consistently repeat. Thus, a computational solution for automatic 3D landmark placement becomes beneficial.

While prior research has examined and reviewed automatic facial landmark detection with 2D images [3], the focus of this paper is 3D landmark placement using 3D facial surface models. Most of the 3D landmark placement methods are based on 3D geometry of the face surface and their associated texture images.

3D shape features are typically computed and used to estimate the initial locations of the landmarks [4][5][6], but the accuracies of these methods are often unsatisfactory due to the lack of a uniform geometric patterns for these landmarks, thereby presenting challenges for 3D facial landmark registration. Combining 3D geometry and their texture images can sometimes improve performance [7][8][9]. There have also been techniques that consider the landmark set as a whole to take better advantage of the overall landmark structures [7][10][11]. Statistical models have been built to estimate landmarks coarsely, and heuristics are then applied to refine the locations [10]. The statistical model [12] combines both structural relationship and local geometric properties.

Shape or image feature based landmark detection methods are known to be less accurate, thus requiring additional refinement. An effective refinement strategy that has gained increasing popularity in recent years is to use machine-learning techniques [13][14][15]. In this approach, the machine-learning algorithm will estimate a model for landmark placement by learning from a set of training faces with manually placed landmarks. This trained model can then be used to automatically adjust and refine the positions of the initially placed landmark points. This approach, however, requires a large number of training faces with manually selected landmarks. As stated earlier, this solution is often not feasible as manually selecting landmarks for a large number of training face images is extremely time-consuming. The challenge is: how to effectively find the landmark placement patterns without the need for a large training set.

To overcome this challenge, we propose a visual analytics approach that takes advantage of human interaction and visual pattern detection. This method's ability to establish patterns and parameters for each individual landmark point, based solely on a user's initial interaction, make it a highly robust method. A substantial advantage of this approach is that only a small number of training faces are needed for a human user to determine the appropriate patterns and their parameters, which can then be used to carry out the automatic landmark refinement process for implementation across datasets with thousands of facial images.

The computational solution presented in this paper is part of a larger effort to establish biological links between human genetics (genotype) and associated facial features (phenotype) in a cohort of more than 5000 individuals. All human traits have a substantial genetic component, including facial features [16] and other outwardly physical appearances such as pigmentation [17]. Such associations can be very useful in a variety of different applications in the medical and forensic sciences. For example, one possible application is the prediction of facial features from DNA using genetic material obtained from a crime scene for criminal investigations.

II. METHOD

A. Overview

In this work, we propose a new visual analytics approach for the automatic placement of 3D facial landmarks. Using this approach, we apply human interaction through the use of human visual pattern learning to determine each landmark's individual local geometric pattern and parameters using a small set of training faces. The main advantage of our approach over machine learning based methods is that only a small set of training samples are required, so that the process of manual landmarking for the training samples is greatly reduced.

Our algorithm first takes a set of 3D facial images of different human subjects obtained using a Canfield Vectra H1 handheld 3D imaging system. 3D stereophotogrammetry utilizes multiple 2D images taken from different positions to estimate the three dimensions of the points so that a 3D image can be rendered. A pre-defined set of anthropological facial landmarks are manually placed on these multiple 2D images during 3D image generation. A random 3D face, along with its landmarks, is chosen as a *template face*, which is then used to align all other 3D faces to generate the initial landmark positions. The remaining 3D faces are subsequently divided into two subsets: a *training set* and a *test set* (80:20).

The first step is to generate a set of local geometric patterns and parameters for each individual landmark point. This is done by visually comparing the local distance field of each manually selected landmark across all training set images to determine a common and representative pattern. To further refine the parameters for each landmark's local geometric patterns, we apply an iterative closest point (ICP) algorithm to align the template face to each face in the training set. The landmarks of the template face can then be projected (as closest points) onto the faces in the training set. Next, the local geometric pattern of each landmark is used to adjust each initial landmark location within its neighborhood until it finds a position that best fits the geometric pattern. We utilize several different pattern sizes and neighborhoods to detect the best sizes as the pattern parameters, which does vary for different landmark points. Finally, these patterns (with chosen parameters) are applied to the test set to validate the results. Fig. 1 shows the overall flow of this algorithm.
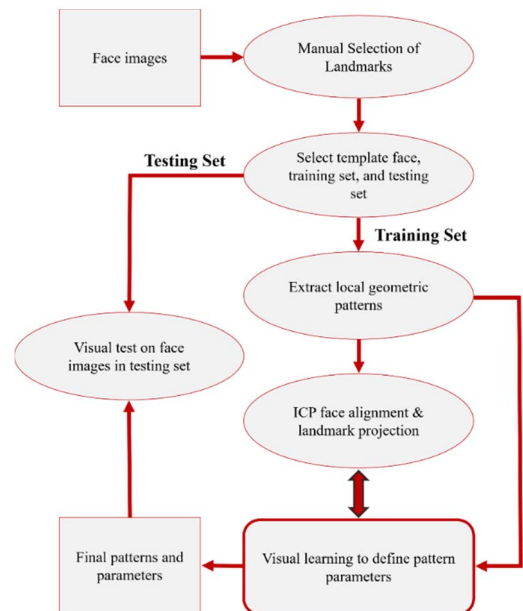

Fig. 1. Control flow of the algorithm

B. Anthropological Facial Landmark Selection

The landmark points on the face used in this study were selectively chosen from standard anthropological landmarks used by Howell and Stephan [18][19], among others. These points include both facial skeleton and soft tissue representations. The framework for the midline and bi-lateral portions of the face were accounted for by incorporating the 23 landmarks (including right and left sides for bi-lateral points) presented in Table 1.

These landmarks were manually placed on three (front, left and right) 2D images of each subject face. These 2D images are used as textures of the 3D polygon mesh surface. The coordinates of the landmarks on the 2D images are considered the texture coordinates of the 3D points on the polygon surface. Thus, to find the 3D point corresponding to a landmark on a 2D image, we only need to search for the 3D vertex that has texture coordinates closest to the 2D image coordinates.

TABLE I. A CURRENT WORKING LIST OF ANTHROPOLOGICAL FACIAL LANDMARKS SELECTED FROM HOWELL AND STEPHAN, INDEPENDENTLY.

Midline Landmarks	Midline Abbreviation	Bi-lateral Landmarks	Bi-lateral Abbreviation (Left/Right)
Glabella	G	Mid-Supraorbital	MSOL/R
Nasion	N	Mid-Infraorbital	MIOL/R
Subnasale	SN	Ectoconchion	ECTL/R
Labarale superius	LS	Dacryon	DACL/R
Infradentale/labarale inferius	LI	Zygion	ZL/R
Mentolabial sulcus	MLS	Alare curvature point	ACPL/R
Pogonion	PG	Gonion	GOL/R
Gnathion	GN		
Menton	M		

C. Extracting Local Geometric Patterns

For a landmark point (vertex) in a 3D polygon mesh surface, a local geometric pattern is defined as a k by k image representing the distances of points in the neighborhood of the vertex to its tangent plane. It can also be called a signed distance field [20] as the distances to the tangent plane can be positive or negative depending on whether the point is above (outside) or below (inside) the plane.

To generate an image from a set of discrete neighborhood distance values, we use a scattered data interpolation method, Shepard interpolation [21], to interpolate the values for each image pixel. As a pattern parameter, the size of the image, k, represents the image resolution of the distance field. Another parameter is the size of the neighborhood, L, on the mesh surface, representing how many times the neighborhood is expanded outwards the landmark vertex. It measures the complexity of the landmark's local geometric landscape. At this stage, multiple k and L values are used to generate multiple pattern images so that the right pattern can be determined later through visual learning.

D. Pattern Image Determination

For each manually placed landmark point and its pair of parameter values (k, L), one image is created for each sample face in the training set. In a perfect world, this image will be the same for all faces in the training set. For various reasons (e.g. landmark selection errors, face differences, etc.), the pattern images can vary across different faces. The first visual learning task is to visually examine these pattern images for each landmark to generate one image that best represents the geometric characteristics of the neighborhood. We start this process by first eliminating outlier images, which are very different from the majority of the others. We can then either average the rest of the images, or simply pick one that is more typical for the given landmark. Fig. 2 shows an example of pattern images for two landmarks: ZL and ZR. Clearly, ZL-C, ZL-D and ZR-C are outliers. The final patterns can be the averages of the rest for each landmark. We may also decide that ZL-B and ZR-D are the more typical ones that should be used based on what we see from the pattern images and the face surface geometry around the landmark points.
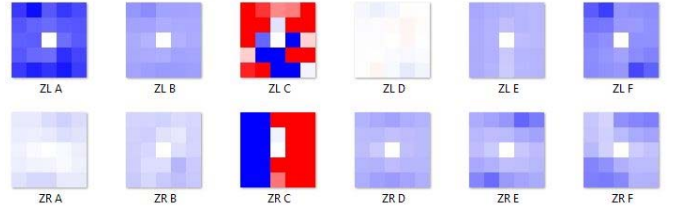

Fig. 2. Pattern images of two landmarks, ZL and ZR

E. Face Alignment by ICP

To generate the initial landmark positions, we apply an ICP alignment technique to project landmark points from a template face to all other faces. A template face, T, is first randomly chosen, which already has landmarks manually placed. For each new face, F, the Iterative Closest Point (ICP) algorithm [22] is applied to align T and F. The ICP algorithm computes an optimal affine transformation (translation, rotation, and scaling) such that the sum of the pairwise distances between each transformed vertex in T and its closest vertex in F is minimized.

Once T and F are aligned, we can project all the landmarks (after ICP transformation) of T onto the surface of F. A projection of a landmark point in T is the closest vertex in F to this landmark point after ICP. These projections are then considered the initial coarse locations of the landmarks of face F. Using this technique, we can generate a set of initial landmarks for every face in the training set and test set, which will later be refined and adjusted.

F. Landmark Refinement and Pattern Parameters

Once the initial landmarks are generated for all faces in the training set, we can apply the landmark pattern images (of various sizes) to further refine these landmarks for faces in the training set. The refined landmark positions can be compared with the manually selected landmarks to evaluate which pattern image (i.e. which parameters, k and L) is the best for each landmark point.

This parameter selection process is again done through human interaction to facilitate holistic visual learning. Using each pattern image, the refinement algorithm will search within the L neighborhood of the initial location of a landmark to find the best match to the pattern image. Since each landmark location on a face is unique, the differences in complexity and delicacy of the landmark neighborhoods require different parameters (k, L) of the pattern images to achieve the best refinement results. The user can make an intuitive decision on

which parameters to try based on what the user sees around the landmarks to selectively improve refinement results.

In addition to pattern image resolution and neighborhood size, a midline constraint can also be applied to those landmarks that should be on the midline of the face. Fig. 3 shows several different neighborhood sizes and image resolutions for one landmark point.

This process generates an individualized pattern metric for each landmark that can be used to refine the initial landmark position. The refinement is done by moving the initial landmark position around its neighborhood (defined by "L") to seek the point with the best matching neighborhood pattern image. If the midline constraint exists for this landmark, the constraint will be applied first to points in the neighborhood, i.e. only points that satisfy the midline constraint will be tested for pattern matching.
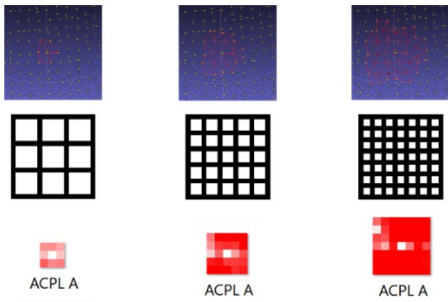

Fig. 3.   Three different sizes of the local geometric patterns

III. EXPERIMENTAL RESULTS

In our experiment, 39 3D facial images with manually selected landmarks were made available. Individuals of African, Asian, European, South American, and Middle Eastern ancestry, a wide range of body mass index (BMI), a variety of ages, and a nearly equal sex distribution were used. Without statistically correcting for these covariates, we illustrate the raw capability of x, y, z coordinate placement of the human observers and the visual analytics approach (VAA) in Fig. 4.

Of the 39 faces, one face was chosen as the template face. We also randomly selected eight faces as the test set. The remaining 30 faces were used as the training set. To ensure accuracy and consistency of the landmark selection process, the landmarks were independently placed by an anthropologist and a student, using an in-house manual coordinate placement program on three 2D texture maps for all faces. 23 anthropological landmarks were defined on each face. Since anthropologists are deemed the experts in anatomical facial landmarking, the anthropologist's landmark coordinates were used as the final points for training the automated algorithm. One caveat of manual landmarking is the need to converge multiple 2D texture map coordinates into a single 3D vertex for each 3D landmark indication. In this intermediary step, it is clear that several manual landmarks (green) are slightly misaligned (Fig. 4D) versus the observer's initial placement. Therefore, accuracy measures of automated versus manual performance may be over-estimated. However, worthy to note, the VAA appears to be robust enough to correct for this error due to its landmark refinement capabilities.
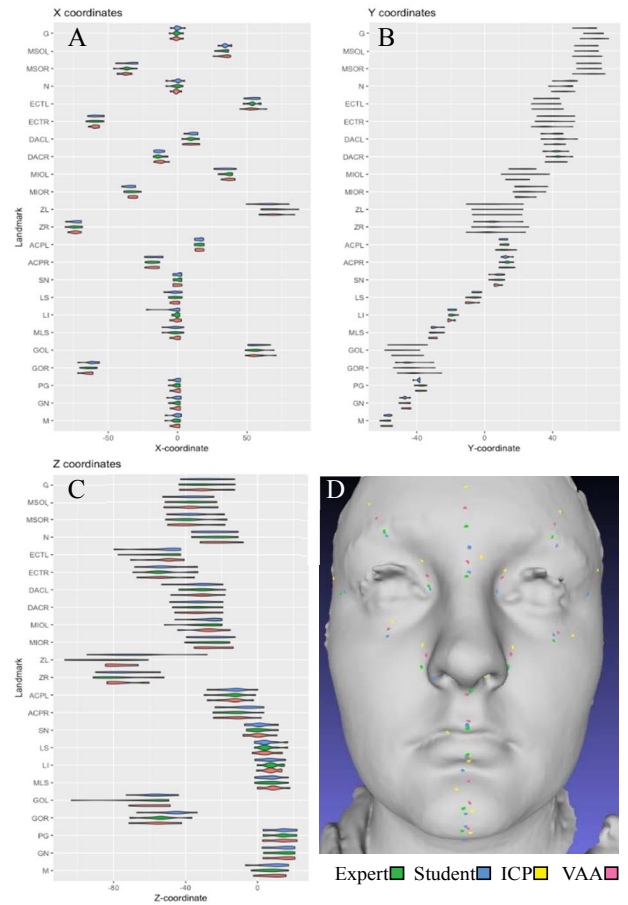

Fig. 4.   X, Y, Z coordinate placement for testing set of facial images. (A), (B), and (C) are the distributions of the x, y, z coordinates, respectively, for each of the observers' manual placement as well as the auto landmark placement (VAA) represented via violin plots. (D) An example of 3D landmark placements on one of the eight test set face images landmark point colors correspond with graphs in (A)-(C). The manual observer landmarks are placed using the 2D texture map to 3D vertex conversions.

As described in the Method section, the 30 training faces were used to generate the 23 pattern images using a visual analytics process, as shown in Fig. 5. The varying resolutions of these images reflect the different image parameters of these patterns.
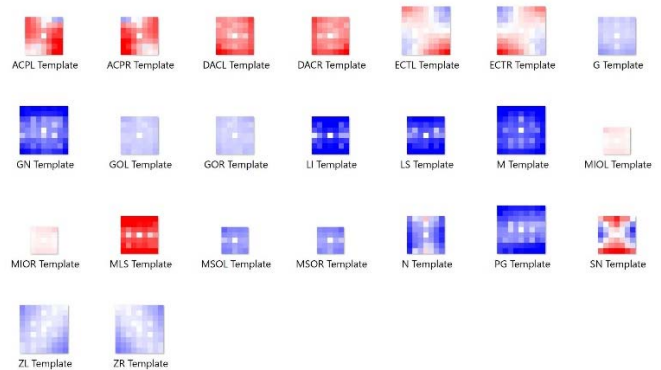

Fig. 5.   Local geometric patterns for all 23 landmarks

For each face in the test set, we first applied ICP to project the landmarks on the template face to the test face. The local geometric patterns, along with their midline constraints, were employed to refine the projected landmark points to generate the final landmark coordinates. To visually compare the results from manual selection of Expert and Student observers, ICP projection, and refined final coordinates (VAA), we plotted all four sets of landmarks on each of the test faces.

Fig. 4D shows the visual interface and the landmark placements for one of the test set face images. In the figure, green and blue dots represent the manually selected points by the Expert and Student, respectively, yellow dots represent the projected points after ICP, and pink dots represent the refined points using their local geometric patterns or VAA. In comparison to ICP points, almost all of the VAA points are closer to the manually placed Expert training points. In many cases, the automatic VAA landmarks can be more accurate than those manually selected, as they may have implicitly corrected potential manual errors using the local geometric patterns or the midline constraint.

In order to quantitatively assess each landmark placement, we set out to compare the differences between the raw X, Y, Z coordinates (Fig. 4A-C) for the Expert, Student, and VAA landmark indications on the testing set images. We calculated the average differences of these X, Y, Z coordinates per landmark on each face to obtain a singular landmark difference. We then averaged each landmark's singular difference across the test set to evaluate individual landmark placement. Fig. 6 visualizes these average differences for the midline and bi-lateral landmarks for the VAA vs. Expert and Student vs. Expert comparisons. The most accurate landmark placements are depicted by the smaller averages where a difference of zero would be an exact match with the Expert placement. This comparison between the Student placement and VAA placement illustrates VAA's ability to landmark closer to the Expert's placement than a student observer at 11 of the 23 landmarks.
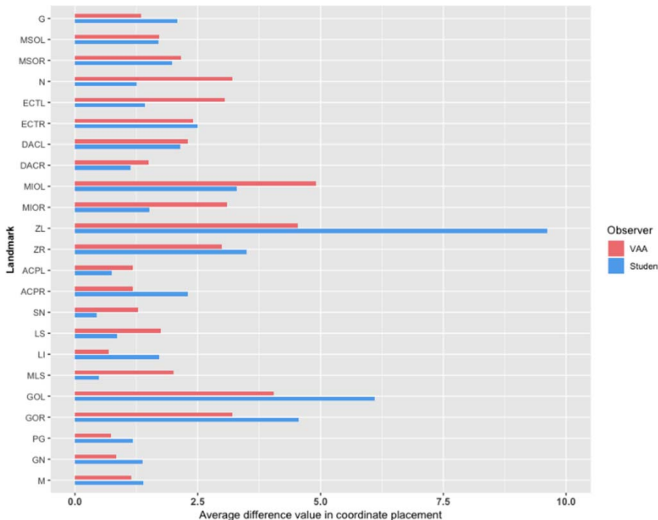

Fig. 6. The difference in the absolute value for each x, y, z coordinate was compared between VAA vs Expert (top/pink) and Student vs Expert (bottom/blue) per landmark across all faces. An average of the singular difference score for midline and bi-lateral landmark differences across the test set was calculated to visualize error amongst the Student and VAA observers.

As evident in Fig. 6, the midline points, overall, tend to exhibit less error for both Student and VAA landmark placement than the bi-lateral points. The average across all of the landmarks per observer was also calculated to determine the overall best performer in terms of less error (difference). The VAA total face average difference value, 2.23, was smaller than that of the Student total face average difference value, 2.32. Overall, the VAA performance is comparable to the Student, and while it is not significantly more accurate at all landmarks, it is much less time-consuming since it can be deployed on datasets containing thousands of 3D facial images.

The internal algorithmic refinement is demonstrated in Table 2 by the closer placement of the refined VAA points (measured against the Expert's manually selected points) than those of the ICP projected points. Table 2 also presents the individualized pattern parameters including pattern image size, neighborhood size, and midline constraint for all 23 landmarks. It should be noted that manually selected points can also have errors, likely from the aforementioned 2D coordinate to 3D vertex convergence. Sometimes those errors can be corrected by the refinement process as the local geometric patterns provide additional local shape information. Biologically speaking, the smaller errors between VAA and Expert suggest that landmarks (e.g. LI or PG, among others) share common topographical features across a wide range of unadjusted covariates such as ancestry, BMI, age, and/or sex.

TABLE II. EUCLIDEAN DISTANCE DIFFERENCES OF THE LANDMARK PLACEMENT AND THEIR PATTERN PARAMETERS TO EVALUATE INTERNAL IMPROVEMENT FROM ICP USING VAA

Landmark	VAA vs Expert	ICP vs Expert	Pattern Size: K	Neighborsize: L	Midline
G	2.87	5.89	7	3	Yes
MSOL	3.45	7.04	5	2	No
MSOR	4.15	7.32	5	2	No
N	6.17	10.09	7	3	Yes
ECTL	5.93	10.99	9	4	No
ECTR	4.53	8.56	9	4	No
DACL	4.71	6.91	7	3	No
DACR	3.26	5.02	7	3	No
MIOL	7.9	13.87	5	2	No
MIOR	5.91	10.29	5	2	No
ZL	5.7	10.27	9	4	No
ZR	6.17	9.22	9	4	No
ACPL	2.46	4.6	7	3	No
ACPR	2.41	4.72	7	3	No
SN	2.52	3.91	7	3	Yes
LS	3.84	7.31	7	3	Yes
LI	1.52	1.97	7	3	Yes
MLS	4.25	5.97	7	3	Yes
GOL	4.09	7.65	7	3	No
GOR	6.03	11.55	7	3	No
PG	1.58	2.79	9	4	Yes
GN	1.89	3.25	9	4	Yes
M	2.32	3.45	9	4	Yes

IV. CONCLUSIONS

In this paper we proposed a visual analytics approach for the automatic placement of 3D facial landmarks. The main advantage of our approach is that it does not require a large training set as do many machine learning techniques. This significantly reduces manual effort of landmark selection by experts, which can be very time-consuming and expensive. Visual analytics approaches take advantage of human abilities in pattern detection and can be very effective and accurate with only a small number of training samples. The local geometric patterns and their parameters are derived interactively by the

user. Although the process involves human decisions, it is a one-time effort and the results can be applied automatically to thousands of face images in the analysis process. Our experiment shows that this approach is efficient, robust and inexpensive. Since the manual landmarking consisted of three, 2D texture maps with coordinate conversion to a 3D vertex, there were obvious manual landmark misplacement, giving rise to possibly larger error values than there should be. Despite this, the user defined local geometric patterns can often correct errors in manually selected landmark points, which indicates that the automatic approach can be even more accurate than human selections. While the patterns and their parameters derived in this paper only apply to our 23 anthropological landmarks, the general principal can be used for any shape-based landmark definitions in other facial or non-facial applications.

REFERENCES

[1] W. Zhao, R. Chellappa, PJ Phillips, A Rosenfeld. Face Recognition: A Literature Survey. ACM Computing Surveys, Vol. 35, No. 4, December 2003, pp. 399–458.

[2] J.T. Richtsmeier and S. Lele. A Coordinate-Free Approach to the Analysis of Growth Patterns: Models and Theoretical Considerations. Biol. Rev. (1993), 68, pp. 381-411.

[3] Yue Wu, Qiang Ji. Facial Landmark Detection: A Literature Survey. International Journal of Computer Vision, May, 2018.

[4] D'Hose, J.; Colineau, J.; Bichon, C.; Dorizzi, B. Precise Localization of Landmarks on 3D Faces using Gabor Wavelets. In Proceedings of the IEEE International Conference on Biometrics: Theory, Applications, and Systems, Crystal City, VA, USA, 27–29 September 2007; pp. 1–6.

[5] Colbry, D.; Stockman, G.; Jain, A. Detection of Anchor Points for 3D Face Verification. In Proceedings of the IEEE Computer Society Conference on Computer Vision and Pattern Recognition, San Diego, CA, USA, 20–25 June 2005.

[6] Dibeklioglu, H.; Salah, A.A.; Akarun, L. 3D Facial Landmarking under Expression, Pose, and Occlusion Variations. In Proceedings of the IEEE International Conference on Biometrics: Theory, Applications and Systems, Arlington, VA, USA, 29 September–1 October 2008; pp. 1–6.

[7] Jahanbin, S.; Choi, H.; Jahanbin, R.; Bovik, A.C. Automated facial feature detection and face recognition using Gabor features on range and portrait images. In Proceedings of the IEEE International Conference on Image Processing, San Diego, CA, USA, 12–15 October 2008; pp. 2768–2771.

[8] Wang, Y.; Chua, C.S.; Ho, Y.K. Facial feature detection and face recognition from 2D and 3D images. Pattern Recognit. Lett. 2002, 23, 1191–1202.

[9] Lu, X.; Jain, A.K. Automatic Feature Extraction for Multiview 3D Face Recognition. In Proceedings of the International Conference on Automatic Face and Gesture Recognition, Southampton, UK, 10–12 April 2006; pp. 585–590.

[10] Nair, P.; Cavallaro, A. 3-D Face Detection, Landmark Localization, and Registration Using a Point Distribution Model. IEEE Trans. Multimedia 2009, 11, 611–623.

[11] Boehnen, C.; Russ, T. A Fast Multi-Modal Approach to Facial Feature Detection. In Proceedings of the Seventh IEEE Workshops on Application of Computer Vision, Breckenridge, CO, USA, 5–7 January 2005; pp. 135–142.

[12] Zhao, X.; Dellandréa, E.; Chen, L.; Kakadiaris, I.A. Accurate landmarking of three-dimensional facial data in the presence of facial expressions and occlusions using a three-dimensional statistical facial feature model. IEEE Trans. Syst. Man Cybern. Part B Cybern. 2011, 41, 1417–1428.

[13] Sun, Y.; Wang, X.; Tang, X. Deep Convolutional Network Cascade for Facial Point Detection. In Proceedings of the Computer Vision and Pattern Recognition, Portland, OR, USA, 23–28 June 2013; pp. 3476–3483.

[14] Zhang, J.; Shan, S.; Kan, M.; Chen, X. Coarse-to-Fine Auto-Encoder Networks (CFAN) for Real-Time Face Alignment. In European Conference on Computer Vision; Springer: Cham, Switzerland, 2014; pp. 1–16.

[15] Kai Wang, Xi Zhao, Wanshun Gao and Jianhua Zou. A Coarse-to-Fine Approach for 3D Facial Landmarking by Using Deep Feature Fusion. Symmetry, 2018, 10, 308;

[16] Shaffer JR, Orlova E, Lee MK, Leslie EJ, Raffensperger ZD, Heike CL, et al. (2016) Genome-Wide Association Study Reveals Multiple Loci Influencing Normal Human Facial Morphology. PLoS Genet 12(8): e1006149. https://doi.org/10.1371/journal.pgen.1006149

[17] S. Walsh, L. Chaitanya, K. Breslin, C. Muralidharan, A. Bronikowska, E. Pospiech, J. Koller, L. Kovatsi, A. Wollstein, W. Branicki, F. Liu, M. Kayser, Global skin colour prediction from DNA. Human Genetics, 2017. 136(7): p. 847-863

[18] Howells, W. W. (1973). Cranial variation in man: a study by multivariate analysis of patterns of difference among recent human populations. Peabody Museum of Archaeology and Ethnology, Harvard Univ.

[19] Stephan, C. N., & Simpson, E. K. (2008). Facial soft tissue depths in craniofacial identification (part I): an analytical review of the published adult data. Journal of Forensic Sciences, 53(6), 1257-1272.

[20] Andreas Bærentzen, J & Aanæs, Henrik. Generating Signed Distance Fields From Triangle Meshes. IMM-TECHNICAL REPORT-2002-21.

[21] Cozac, I. (2003). Shepard Method - From Approximation to Interpolation. Studia University "Babes - Bolyai", Mathematica, XLVIII(2), 49-52.

[22] Ying, S., Peng, J., Du, S., & Qiao, H. (2009). A Scale Stretch Method Based on ICP for 3D Data Registration. IEEE Transactions on Automation Science and Engineering, 6(3), 559-565.